View Article Online
View Journal

# Dalton Transactions

An international journal of inorganic chemistry

## Accepted Manuscript

This article can be cited before page numbers have been issued, to do this please use: D. E. S. Silva, A. B. Becceneri, J. V. B. Santiago, J. A. G. Neto, J. A. Ellena, M. R. Cominetti, J. C. M. Pereira, M. J. Hannon and A. Vieira de Godoy Netto, *Dalton Trans.*, 2020, DOI: 10.1039/D0DT01134G.




ROYAL SOCIETY OF CHEMISTRY

rsc.li/dalton

View Article Online
DOI: 10.1039/D0DT01134G

ARTICLE

# Silver(I) complexes of 3-methoxy-4-hydroxybenzaldehyde thiosemicarbazones and triphenylphosphine: structural, cytotoxic and apoptotic studies

Received 00th January 20xx,
Accepted 00th January 20xx

DOI: 10.1039/x0xx00000x

Débora E. S. Silva,[a] ✉ Amanda B. Becceneri,[b] João V. B. Santiago,[a] José A. Gomes Neto,[a] Javier Ellena,[c] Márcia R. Cominetti,[b] José C. M. Pereira,[a] Michael J. Hannon[d] and Adelino V. G. Netto[a] ✉

Novel silver(I) complexes of the type $[AgCl(PPh_3)_2(L)]$ {$PPh_3$ = triphenylphosphine; L= VTSC = 3-methoxy-4-hydroxybenzaldehyde thiosemicarbazone (**1**); VMTSC = 3-methoxy-4-[2-(morpholine-1-yl)ethoxy)benzaldehyde thiosemicarbazone (**2**); VPTSC = 3-methoxy-4-[2-(piperidine-1-yl)ethoxy)benzaldehyde thiosemicarbazone (**3**)} were synthesized and fully characterized by spectroscopic techniques. The molecular structures of complexes **2** and **3** were determined by single crystal X-ray diffraction. The compounds **1-3** exhibited appreciable cytotoxic activity against human tumor cells (lung A549, breast MDA-MB-231 and MCF-7) with $IC_{50}$ values in 48 h of incubation ranging from 5.6 to 18 μM. Cellular uptake studies showed that complexes **1-3** were efficiently internalized after 3 hours of treatment in MDA-MB-231 cells. The effects of complex **1** in cell morphology, cell cycle, induction of apoptosis, mitochondrial potential membrane ($\Delta\psi m$) and reactive oxygen species (ROS) production have been evaluated in triple negative breast cancer (TNBC) cells MDA-MB-231. Our results showed that complex **1** induced typical morphological alterations of cell death, an increase in cells at sub-G1 phase, apoptosis and mitochondrial membrane depolarization. Furthermore, DNA binding studies evidenced that **1** can bind to ct-DNA and does so without modifying the B-structure of the DNA, but that the binding is weak compared to Hoechst 33258.

## Introduction

Breast cancer affected more than 2 million women worldwide in 2018 being the leading cause of cancer death.[1] Triple negative breast cancer (TNBC) is the most aggressive breast cancer subtype, comprises about 20% of all cases, and has the shorter overall survival. TNBC is characterized by a lack of expression of estrogen (ER) and progesterone receptors (PR), and does not exhibit amplification of the human epidermal growth factor receptor 2 (HER2).[2] Since no specific molecular targets has been identified for the TNBC, chemotherapy is the main available therapeutic option. However, its limited efficacy makes it crucial to develop new anticancer agents against TNBC.[3]

The anticancer potential of silver-based compounds have attracted considerable interest in the last few decades.[4,5] A growing body of evidence suggests that these complexes generally exert their cytotoxicity by altering the membrane structure, interacting with nucleic acids and inducing oxidative stress.[6] However, their action against tumor cells is strictly dependent on a number of parameters such as solubility and stability in aqueous media/biological medium, rate of release of $Ag^I$, and lipophilicity. Such parameters may be fine-tuned by carefully selecting a suitable set of ligands.[5,7] Among the available ligands, phosphines have been systematically employed in the design of new metal complexes for therapeutic purposes due to its versatility and rich coordination chemistry.[8] In addition, the lipophilic character of phosphines may assist in crossing the cellular membrane, consequently, increasing the cell internalization of the metal compound.[9] Since the pioneering work of Berners-Price and Sadler[10], considerable efforts have been devoted to the investigation of the antitumor potential of silver phosphine complexes. There is a growing number of silver compounds containing the "$Ag(PR_3)_2(L)$" core that have gained increasing attention due to their promising cytotoxic effects on a variety of tumor cells.[11,12,13,14,15,16,17] For instance, Engelbrecht *et al.*[17] have described that $[Ag(SCN)(PR_3)_2]$ ($PR_3$ = tris-4-methoxyphenylphosphine) induced mitochondrial apoptosis in esophageal squamous carcinoma (SNO) cell line. This silver complex was more active

[a] Department of General and Inorganic Chemistry, Department of Analytical Chemistry, UNESP – São Paulo State University, Institute of Chemistry, CEP 14800-060 Araraquara, SP, Brazil. E-mail: deboraeduarda.soares@gmail.com; adelino.netto@unesp.br
[b] Department de Gerontology, Federal University of São Carlos, CEP 13565-905 São Carlos, SP, Brazil.
[c] São Carlos Institute of Physics, University of São Paulo, CEP 13.566-590, São Carlos, SP, Brazil.
[d] School of Chemistry, University of Birmingham, Birmingham, B15 2TT, UK.
[e] † Footnotes relating to the title and/or authors should appear here.
[f] Electronic Supplementary Information (ESI) available: [details of any supplementary information available should be included here]. See DOI: 10.1039/x0xx00000x

than cisplatin and showed reduced toxicity towards two non-malignant cells (dermal and kidney cell lines). Complexes of the type $[Ag(L)(PPh_3)_2]$ (L = benzoic acids; $PPh_3$ = triphenylphosphine) induced apoptosis in leiomyosarcoma (LMS) and human breast adenocarcinoma (MCF-7) cell lines.[16]

Recently, we have studied the cytotoxic and apoptotic effects of compounds of the type $[Ag(phen)(L)]NO_3$ {phen = 1,10-phenantroline; L = 2-formylpyridine-N(4)-R-thiosemicarbazones) on TNBC cell line MDA-MB-231.[18] One of these complexes was not only more active than cisplatin, but also was less toxic for the non-tumor breast cell line MCF-10A. These findings have prompted us to investigate the antitumor potential of new silver compounds obtained by the replacement of 1,10-phenanthroline by triphenylphosphine ($PPh_3$). However, as a result of the enhancement of hydrophobicity caused by $PPh_3$, the metal phosphine complexes tend to be less soluble in polar solvents.[5] Recently, Bisceglie *et al*.[19] have modified thiosemicarbazones with polar groups, such as *N*-ethylmorpholine, aiming the modulation of the lipophilicity/hydrophilicity of metal complexes. In this work, we have used vanillin thiosemicarbazones (3-methoxy-4-hydroxybenzaldehyde thiosemicarbazone) *O*-alkylated with *N*-ethylmorpholine and *N*-ethylpiperidine moieties to enhance the solubility of silver complexes in polar solvents.

In the framework of our ongoing research on new bioactive metal complexes,[20,21,22,23] we report herein the synthesis, cytotoxic and apoptotic studies of new tetrahedral silver(I) compounds of the type $[AgCl(PPh_3)_2(L)]$ {$PPh_3$ = triphenylphosphine; L= VTSC = 3-methoxy-4-hydroxybenzaldehyde thiosemicarbazone (**1**); VMTSC = 3-methoxy-4-[2-(morpholine-1-yl)ethoxy)benzaldehyde thiosemicarbazones (**2**); VPTSC = 3-methoxy-4-[2-(piperidine-1-yl)ethoxy)benzaldehyde thiosemicarbazone (**3**)}. The cytotoxic activities of **1**-**3** were evaluated against breast cancer cell lines MDA-MB-231 (TNBC) and MCF-7 (hormone-responsive) and lung cancer cell line (A549). As a comparison, the toxic effects of silver compounds on non-tumor breast cells (MCF-10A) have also been determined. The effects of **1** on MDA-MB-231 cells regarding cell morphology, apoptosis, cell cycle, reactive oxygen species (ROS) formation and mitochondrial potential membrane ($\Delta\psi m$) have also been investigated. The DNA binding ability of **1** has also been investigated by means of circular dichroism and competitive assays with Hoechst 33258.

## Results and discussion

### Synthesis and characterization

#### Thiosemicarbazones

The synthesis of the new thiosemicarbazones was accomplished using a two-step synthetic protocol: i) *O*-alkylation of the vanillin followed by Schiff-base condensation of the appropriate functionalized aldehyde with thiosemicarbazide, as depicted in Scheme 1. Compounds 3-methoxy-4-[2-(morpholine-1-yl)ethoxy)benzaldehyde (**VM**) and 3-methoxy-4-[2-(piperidine-1-yl)ethoxy)benzaldehyde (**VP**) were prepared by the treatment of the commercially available vanillin with 1-(2-Chloroethyl)morpholine hydrochloride and 1-(2-Chloroethyl)piperidine hydrochloride, respectively. The new compounds **VMTSC** and **VPTSC** were obtained as microcrystalline solids in good yields (70-80%) by the condensation of thiosemicarbazide and aldehydes **VM** and **VP**, respectively, in the presence of HCl as catalyst. Compounds **VMTSC** and **VPTSC** were further analyzed using elemental analyses, IR spectroscopy, $^1$H, COSY, $^1$H-$^{13}$C HSQC and HMBC NMR spectroscopy. The details of the synthetic procedures and structural characterization are described in the Experimental Section. The purity of the compounds **VMTSC** and **VPTSC** was further confirmed by elemental analysis. The condensation of thiosemicarbazide and functionalized aldehydes was confirmed by the disappearance of the characteristic νCO bands at ca. 1700 cm$^{-1}$ in the IR spectra of **VM** and **VP** together with the appearance of the typical absorptions from thiosemicarbazone moiety at ca. 3170 cm$^{-1}$ (νNH), 1600 cm$^{-1}$ (νCN) and 758 – 780 cm$^{-1}$ (νCS).[25] The NMR spectra of the thiosemicarbazones **VMTSC** and **VPTSC** were in full agreement with their molecular structure, being observed only one set of signals (see ESI). $^1$H NMR spectra of **VMTSC** and **VPTSC** clearly exhibited the typical signals of thiosemicarbazone moiety: a singlet at 11.31 ppm (=N-NH-), two broad signals at ca. 8.2 – 8.0 ppm (-$NH_2$) and a singlet at 7.95 ppm (-HC=N).[25] Besides the expected signals of piperidine and morpholine groups, $^1$H NMR spectra also showed the characteristic signals for ethylene groups and vanillin over the spectral range of 4.1-2.6 and 7.5-7.0 ppm, respectively. Integration of the proton signals was in accord with the requirements for **VMTSC** and **VPTSC**. The most important feature of DEPTQ spectra is the appearance of a low field resonance at ca. 142.5 ppm which was assigned to the iminyl carbon [-HC=N-] together with the presence of the thiocarbonyl group signal (C=S) at 177.5 ppm.

#### Silver(I) compounds

The complexes **1-3** were synthesized from the reaction of AgCl with 3-methoxy-4-R-benzaldehyde thiosemicarbazone and $PPh_3$ = triphenylphosphine in a 1:1:2 molar ratio, respectively (Scheme 1). The compounds were characterized by IR and NMR spectroscopy, elemental analysis and single-crystal X-ray diffraction. Microanalysis data confirmed the expected formulation. The IR spectra of **1–3** showed characteristics bands at 1600 ν(C=N) and 745 ν(C=S) cm$^{-1}$ from thiosemicarbazones. The shift of the C=S band from 758-780 cm$^{-1}$ (free ligands) to lower frequency suggested the coordination via sulfur atom.[25] In addition, no shift of the ν(C=N) absorption was noticed, supporting the S-monodentate coordination in the solid state. The presence of intense absorption at 1095 cm$^{-1}$ evidenced coordination of triphenylphosphine in the compounds **1-3**.[26]

The molecular structures of complexes **2** and **3** were determined by single-crystal X-ray diffraction (Fig. 1). The crystallographic data and selected bond parameters are listed in Tables 1 and S1, respectively. Both complexes crystalize in the monoclinic space group I2/a with one chlorine, one sulfur atom of the thiosemicarbazone and two phosphorous from two triphenylphosphine molecules coordinated to the silver(I) atom.

View Article Online
DOI: 10.1039/D0DT01134G

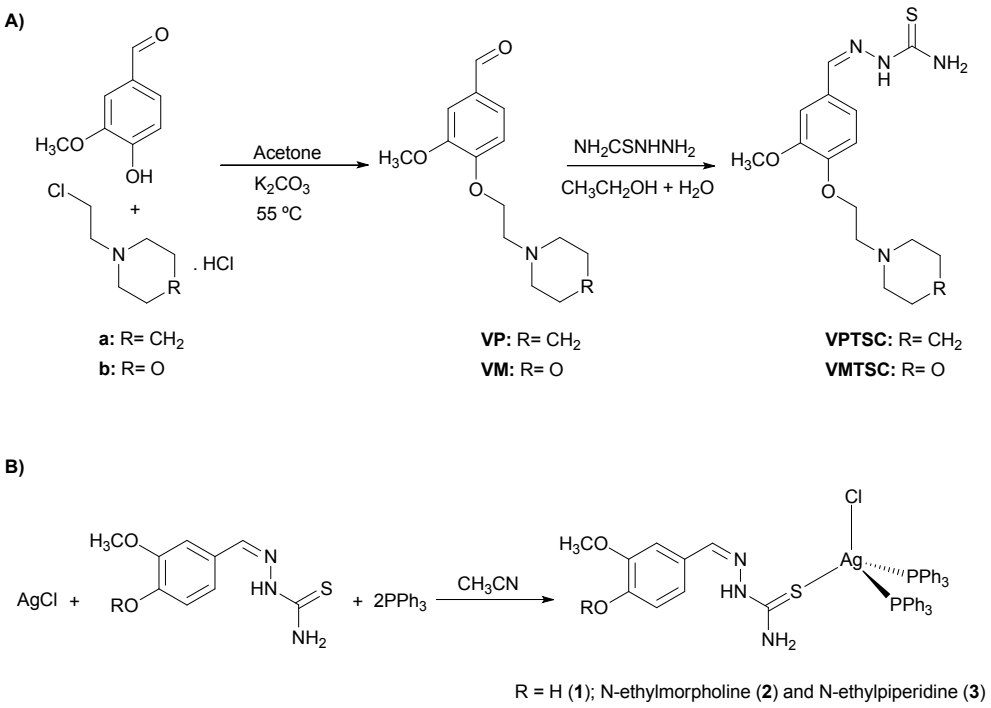


**Scheme 1** Reaction scheme of (A) thiosemicarbazones and (B) silver(I) compounds.

The metal coordination form a distorted tetrahedral with bond angles ranging from 99.8° to 124.21°. The Ag-S bond length are 2.6013 Å and 2.6325 Å in **2** and **3**, respectively, which are close to that reported ones for similar silver complexes [AgCl(κ$^1$-S-L)(PPh$_3$)$_2$] (L=pyridine-2-carbaldehyde thiosemicarbazone) and [AgCl(η1-S-HIntsc)(Ph$_3$P)$_2$] (HIntsc = indole-N1-methyl-3-thiosemicarbazone) with neutral monodentate thiosemicarbazones.[27,28] The Ag-P bond lengths in complexes **2** and **3** are comparable to those observed for similar complexes in the literature.[27,28] The chloride ligand is involved in intramolecular hydrogen bonding with the NH of thiosemicarbazone, leading to the formation of six membered ring.

**Solution studies**

$^1$H and DEPTQ NMR spectra of complexes **1-3** in DMSO-d$_6$ showed all the expected signals and integration. Upon coordination, the hydrazinic proton (=N-NH$^2$) signal was shifted ca. 0.3-0.4 ppm to downfield, suggesting that thiosemicarbazones act as neutral ligands. The iminyl-HC=N signal did not change significantly after complexation. In the DEPTQ NMR spectra of **1-3**, the C=S signal was displaced ca. 1.1-1.5 ppm upfield compared to the free thiosemicarbazones, indicating a weakening of the C=S bond as a result of the Ag-S bond formation.[29] A downfield shifted of ca. 1.0-1.3 ppm was noticed for the azomethine carbon resonance (-HC=N) upon coordination, which suggested the coordination of imine nitrogen to silver(I) ion. This finding may indicate that thiosemicarbazone acts as a *N,S*-ligand in solution. The signals assignable to the vanillin aromatic protons (H2, H5, H6), methoxyl group, and N-ethylmorpholinyl/piperidinyl moieties were not affected on coordination. The typical resonances of triphenylphosphine protons were noticed in the range of 7.33 – 7.43 ppm. The $^{31}$P NMR spectra of complexes **1-3** in DMSO-d$_6$ exhibited one singlet at δ 4.8 – 2.9 ppm at 298 K because of the rapid intermolecular exchange of the PPh$_3$ ligands, which is a well-documented behavior for phosphine based complexes of coinage metals.[30,31,32]

In order to evaluate the stability of **1**-**3** under biologically relevant conditions, we have conducted some time-dependent experiments in solution phase. Due to their low aqueous solubility, **1**-**3** were dissolved in a mixture of DMSO-d$_6$/D$_2$O (80:20%, v/v) and their $^1$H NMR spectra were collected at 0, 24 and 48 h after sample preparation (Fig. S13). At 0 h, the aromatic region of the spectra of **1** and **2** (Figure S13) exhibited a complex multiplet from PPh$_3$ ligands centred at 7.24 ppm which became relatively more resolved at 24 h and remained unchanged at 48 h. This finding may be associated with a change of the coordination mode of thiosemicarbazone in solution. No significant spectral changes were noticed over this period for **3**. In all cases, no signals assignable to the free ligands were detected over this period. UV-Vis spectra of the silver complexes **1**-**3** in Tris-HCl buffer (pH 7.4, [Cl$^-$] = 50 mM, 2% DMSO, 298 K) were also registered at 0, 24 and 48 h (Fig. S14). Over the 48-h period in Tris-HCl buffer, the CT band (ca. 321 nm) decreased in intensity (15-37%), which may indicate that a considerable amount of the silver complexes remained intact in the presence of Cl$^-$.

View Article Online
DOI: 10.1039/D0DT01134G

**Table 1** Crystallographic data and experimental details for complexes **2** and **3**.

| | **2** | **3** |
|---|---|---|
| CCD Number | 1992316 | 1992321 |
| Empirical formula | $C_{51}H_{52}AgClN_4O_3P_2S$ | $C_{47}H_{49}AgCl_2N_6O_2P_2 \cdot 0.13C_2H_3$ |
| Formula weight | 1016.69 | 974.64 |
| Temperature (K) | 293(2) | 298 |
| Crystal system | monoclinic | monoclinic |
| Space group | I2/a | I2/a |
| a (Å) | 25.4270(9) | 25.5169(10) |
| b (Å) | 12.1243(5) | 10.2681(3) |
| c (Å) | 33.2299(10) | 43.6410(13) |
| α (°) | 90 | 90 |
| β (°) | 100.785(3) | 102.951(3) |
| γ (°) | 90 | 90 |
| Volume (Å$^3$) | 10063.3(6) | 11143.5(7) |
| Z | 8 | 8 |
| $\rho_{calc}$ (g/cm$^3$) | 1.342 | 1.162 |
| μ (mm$^{-1}$) | 0.621 | 0.557 |
| F(000) | 4200.0 | 4016.0 |
| Crystal size (mm$^3$) | 0.35 × 0.28 × 0.2 | 0.25 × 0.2 × 0.18 |
| Radiation | Mo Kα (λ = 0.71073) | MoKα (λ = 0.71073) |
| 2Θ range for data collection (°) | 5.03 to 55 | 5.098 to 68.974 |
| Index ranges | -32 ≤ h ≤ 33, -15 ≤ k ≤ 13, -42 ≤ l ≤ 43 | -31 ≤ h ≤ 39, -14 ≤ k ≤ 15, -68 ≤ l ≤ 54 |
| Reflections collected | 23269 | 94501 |
| Independent reflections | 11513 [Rint = 0.0257, Rsigma = 0.0390] | 22366 [Rint = 0.0601, Rsigma = 0.0670] |
| Data/restraints/parameters | 11513/0/569 | 22366/0/569 |
| Goodness-of-fit on F2 | 1.060 | 1.010 |
| Final R indexes [I>=2σ (I)] | R1 = 0.0366, wR2 = 0.0722 | R1 = 0.0530, wR2 = 0.1186 |
| Final R indexes [all data] | R1 = 0.0628, wR2 = 0.0882 | R1 = 0.1286, wR2 = 0.1488 |
| Largest diff. peak/hole / e Å$^{-3}$ | 0.45/-0.40 | 0.83/-0.60 |

**Cytotoxic activity**

The cytotoxic activity of vanillin thiosemicarbazones and compounds **1-3** in breast (MCF-7 and MDA-MB-231) and lung (A549) human tumor cells has been evaluated by using the MTT assay after 48 hours of incubation.[33] The $IC_{50}$ values are summarized in Table 2. The assays were also performed with cisplatin under same experimental conditions, as a reference drug. The vanillin thiosemicarbazones **VTSC, VMTSC** and **VPTSC** are not cytotoxic, no drug response was observed at concentrations > 100 μM in all the tested tumor cell lines. On the other hand, the silver(I) compounds **1-3** were more cytotoxic than cisplatin against MDA-MB-231, MCF-7 and A549 cells, with $IC_{50}$ values ranging from 5.63 to 18.80 μM. The compounds **1-3** displayed comparable cytotoxicity, suggesting that the incorporation of *O*-alkylated vanillin thiosemicarbazones did not increase their activity. Particularly, the complex **1** was more cytotoxic in TNBC cells MDA-MB-231 (5.63 ± 0.13 μM) than in hormone sensitive cells MCF-7 (16.63 ± 1.08 μM). As a comparison, the cytotoxic effects of compounds **1-3** were also evaluated towards the non-tumor cell line MCF-10A. The silver(I) compounds exhibited higher selectivity index (SI) values (in the range of 1.3 - 1.7) compared to cisplatin (0.9) (Table 2). It is important to emphasize that silver compounds can take part in competing ligand exchanging reactions with biological components during the cytotoxic experiments, giving rise to new species which may be responsible for the observed activity. Therefore, the $IC_{50}$ values may not reflect rigorously the activity of either the original silver complexes, free ligands or Ag(I) ion.

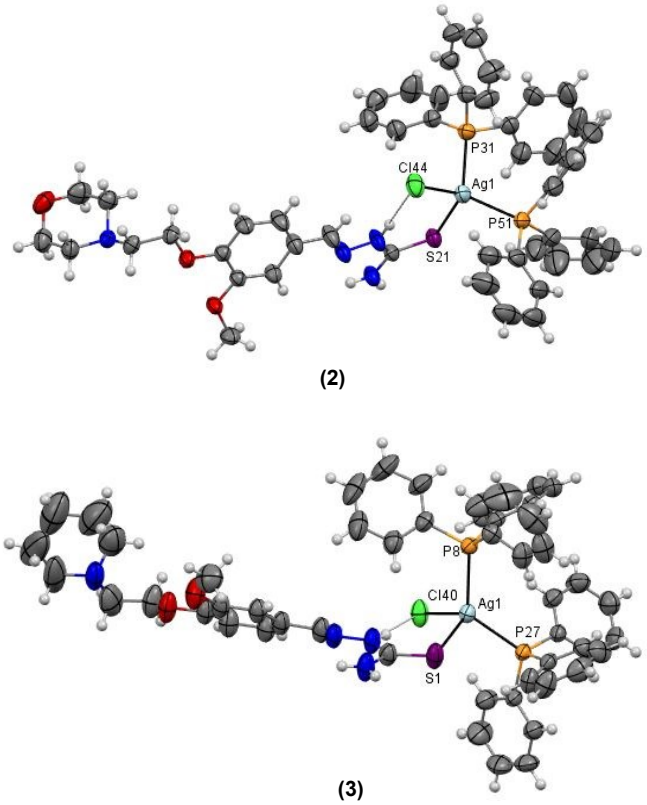


**Fig. 1** Ortep type diagram of the asymmetric unit of the complexes **2** and **3** showing the atomic labelling scheme around the silver(I) atom and ellipsoids at the 50% probability level.

View Article Online
DOI: 10.1039/D0DT01134G

**Table 2** $IC_{50}$ values (μM) of compounds against human tumour cells A549, MCF-7 and MDA-MB-231 and non-tumour breast cells MCF-10A.

| Compound | A549 | MCF-7 | MDA-MB-231 | MCF-10A | SI[a] |
|---|---|---|---|---|---|
| **1** | 7.48 ± 0.21 | 16.63 ± 1.08 | 5.63 ± 0.13 | 8.39 ± 0.11 | 1.5 |
| **2** | 8.15 ± 1.21 | 5.78 ± 0.57 | 6.72 ± 0.46 | 11.61 ± 0.88 | 1.7 |
| **3** | 6.46 ± 0.51 | 18.80 + 0.63 | 7.16 ± 0.10 | 9.53 ± 0.64 | 1.3 |
| VTSC | >100 | >100 | >100 | - | - |
| VMTSC | >100 | >100 | >100 | - | - |
| VPTSC | >100 | >100 | >100 | - | - |
| Cisplatin | 23.36 ± 0.42 | 49.60 ± 3.69 | 43.85 ± 2.4 | 39.12 ± 4.87 | 0.9 |

[a] Selectivity index (SI): $IC_{50}$ MCF-10A/$IC_{50}$ MDA-MB-231





### Cellular uptake

The cellular uptake ability of metal complexes have been related to their cytotoxic activity.[34,35] In this sense, the cellular uptake of complexes **1-3** was evaluated in TNBC cells MDA-MB-231. The Ag uptake was determined in MDA-MB-231 cells exposed to 12 μM of compounds for 3 hours. The initial concentration of Ag in the solutions of complexes **1-3** used to the treatment was also quantified. Based on the initial concentration of **1-3**, the percentage of Ag uptake was calculated. As shown in Fig 2, about 30% of **1-3** added to the cell medium were internalized in MDA-MB-231 cells after 3 hours of incubation. Consistently, the Ag uptake results are in agreement with *in vitro* cytotoxic activity of compounds **1-3**. These results evidenced that the modification of vanillin thiosemicarbazones with *N*-ethylmorpholine and *N*-ethylpiperidine moieties did not improve their cytotoxic effects neither cellular uptake. For comparison purposes, cellular uptake studies on compounds of the type [Ag(phen)(L)]$NO_3$ {phen = 1,10-phenantroline; L = 2-formylpyridine-N(4)-R-thiosemicarbazones) revealed that only 8-12% of them were taken up by MDA-MB-231 cells after 6 hours of incubation.[18] This finding agrees well with previous observation that the lipophilic nature of $PPh_3$ ligands plays an important role in cellular membrane crossing, thus, enhancing the cell internalization of the metal complexes.[9]

### Morphological studies

In order to examine the cytotoxic effects of complex **1** in MDA-MB-231 cells, the cell morphology was analyzed over a period of 48 hours of incubation. As shown in Fig. S15, the untreated cells exhibited normal morphology. On the other hand, the MDA-MB-231 cells treated with **1** showed typical morphological features of cell death. The morphological changes were concentration and time-dependent. MDA-MB-231 cells treated with **1** exhibited a significant decrease in cell density. The treatment for 24 h at 12 and 24 μM induced the appearance of shrunk and round cells. After 48 h, these changes were observed for all tested concentrations. These morphological alterations have been ascribed to cell death via apoptosis.[36,37]

### Cell cycle

Considering that cell cycle arrest may be an effective strategy to inhibit the proliferation of tumor cells,[38] the effect of complex **1** in the cell cycle distribution of MDA-MB-231 cells was investigated. TNBC cells were incubated with 6 μM of **1** for 48 h, stained with propidium iodide (PI) and the DNA content was determined using flow cytometry. The percentage of cell population in each phase is shown in Fig. 3. It was observed a notable increase of the sub-G1 cell population after treatment with complex **1**, evidencing the induction of internucleosomal DNA fragmentation, which is a result of apoptosis.[39] The percentage of cells at sub-G1 phase in the control (5.5%) increased to 23.3% after treatment. Concomitantly, a significant decrease in G1 cell population from 70.4% (control) to 43% and an increase in S cell population from 10.9% (control) to 15%, were also observed in MDA-MB-231 cells treated with complex **1**. The treatment with camptothecin (a pro-apoptotic drug)[40] induced significant effects in the MDA-MB-231 cycle, the sub-G1 cell population increased to 60.6%, whereas G1 and S cell population decreased to 31.1 and 3.7%, respectively (Fig. 3).

### Cell apoptosis

To evaluate the apoptosis induced by the complex **1** in TNBC cells, the Annexin V/ 7-AAD double staining assay was performed. MDA-MB-231 cells were exposed to 6 and 12 μM of **1** for 48 h, stained with Annexin V and 7-AAD and analyzed by flow cytometry. As shown in Fig. 4, the percentage of apoptotic cells significantly increased, after treatment with complex **1**, compared to the control cells. In addition, the percentage of necrosis was insignificant in treated cells. The total percentage of apoptotic cells increased from 10.9% (control) to 69.8% after treatment with 12 μM of **1**. The treatment with camptothecin induced 43.4% of apoptosis in MDA-MB-231 cells (Fig. 4). These results indicated that complex **1** potently induces late apoptosis in MDA-MB-231 cells.

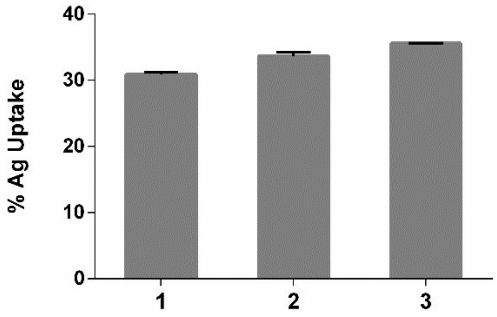


**Fig. 2** Cellular uptake of silver(I) compounds after 3 h of treatment in MDA-MB-231 cells

View Article Online
DOI: 10.1039/D0DT01134G



**The mitochondrial membrane potential (ΔΨm) assay**

In order to verify whether apoptosis induced by the complex **1** in TNBC cells is mediated by the intrinsic pathway, the effects of **1** on mitochondrial membrane potential (ΔΨm) were examined. MDA-MB-231 cells were treated with **1** (6, 12 and 24 μM) for 4 h, stained with JC-1 and analyzed by flow cytometry.[41] JC-1 is mitochondrial fluorescent dye that forms aggregates with red fluorescence in cells with normal mitochondria. On the other hand, in apoptotic cells with damaged mitochondria, the membrane potential decreases, and monomers with green fluorescence can be seen. As shown in Fig. 5, the control cells exhibited red fluorescence. MDA-MB-231 cells treated with complex **1** showed changes in mitochondrial ΔΨm compared to the control cells, indicating the mitochondrial membrane depolarization in a concentration-dependent manner (Fig. 5). In 4 h of treatment at 24 μM of **1**, the percentage of cells emitting green fluorescence increased to 47%, compared to 2.1% in untreated control cells. Cisplatin did not affect the mitochondrial membrane potential in TNBC cells under similar experimental conditions (Fig. 5).

**ROS formation**

The intrinsic apoptosis pathway can be triggered by intracellular ROS generation.[42] In addition, ROS generation has been proposed as common mediator for apoptosis promoted by many metal complexes.[43,44,45] So, as a preliminary study, the intracellular ROS formation was investigated by 2',7'-dichlorodihydrofluorescein diacetate ($H_2$DCFDA) staining. The oxidation of non-fluorescent dye ($H_2$DCFDA) by intracellular ROS produce the fluorescent probe 2',7'-dichlorofluorescein (DCF). The effect of complex **1** on intracellular ROS formation was evaluated in TNBC cells (Fig. 6). MDA-MB-231 cells were exposed to **1** (6 and 12 μM) for 24 h, stained with $H_2$DCFDA and analyzed by confocal fluorescence microscopy. Control cells exhibited no significant green fluorescence. After treatment with **1**, a remarkable increase of green fluorescence in the TNBC cells was observed, demonstrating intracellular ROS formation induced by complex **1**. Cisplatin has also promoted the increase of green fluorescence in the cells (Fig. 6). Our findings may suggest that compound **1** induces an enhancement of intracellular ROS production in the MDA-MB-231 cells, which would be related to apoptotic cell death pathway. However, although $H_2$DCFDA probe is widely employed for detecting intracellular $H_2O_2$ and other oxidants, caution should be taken when interpreting these results. According to Kalyanaraman et al., [46] several limitations are associated with the use of this protocol due to the complex intracellular redox chemistry of HDCF carboxylate anion.

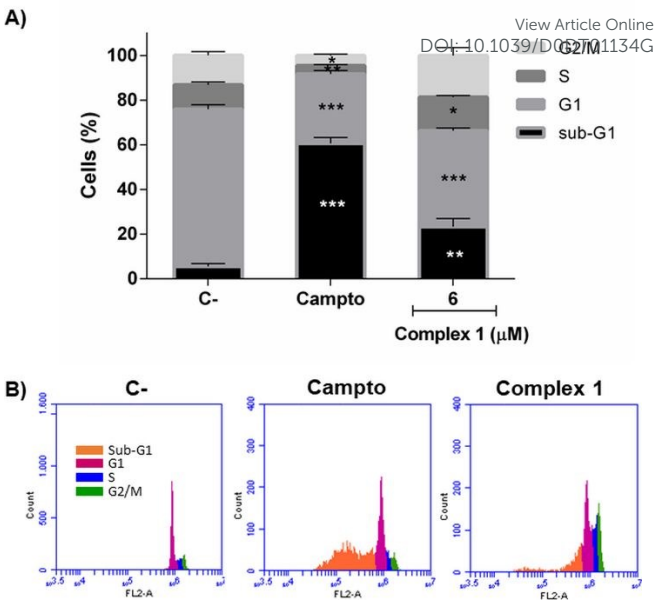


**Fig. 3** A) Effects of complex **1** on MDA-MB-231 cell cycle. TNBC cells were treated for 48 h with **1** (6 μM) or camptothecin (Campto, 20 μM). Data are the mean of experiments in triplicate (*p ≤ 0.01, **p ≤ 0.001 and ***p ≤ 0.0001). B) Representative histograms of cell cycle.

**DNA interaction**

The binding of metal complexes with DNA can be explored using circular dichroism (CD) spectroscopy.[47,48] The CD spectrum of ct-DNA was recorded in the presence of increasing concentrations of **1** (Fig. S16). The typical DNA signature CD spectroscopy was unchanged on addition of complex **1,** confirming that a B-DNA structure is retained when the two species interact. No induced peaks in the complex spectroscopy were observed.

Competitive binding studies with Hoechst 33258 were also performed. Hoechst 33258 binds to the minor groove of DNA and displays a strong fluorescence when bound to DNA.[49] Thus, the quenching of the intrinsic fluorescence of Hoechst-bound DNA upon addition a metal complex can be used to examine whether the metal complex can bind to DNA and displace the Hoechst 33258. Silver(I) complex **1** was titrated into a ct-DNA solution pre-treated with Hoechst 33258, and the emission intensity was recorded. As shown in Fig. S17, the emission intensity of Hoechst-bound DNA at 458 nm decreased by >70% upon addition of **1**, confirming that **1** can bind to DNA and can displace the Hoechst 33258 from the minor groove. Although the displacement of Hoechst is sometimes ascribed to competitive minor groove binding (and this would potentially be feasible for this complex), Hoechst can also be displaced by agents that bind elsewhere on the DNA.[50] While complex **1** can clearly displace Hoechst, it is a less strong binder, and even in presence of a ten-fold excess of complex the Hoechst fluorescence is not completely quenched.

At this point, it seems instructive to make some discussion regarding possible mechanisms, which might account for the cytotoxic effects of silver complexes on MDA-MB-231 cell line.

In our study, the new thiosemicarbazones **VTSC, VMTSC** and **VPTSC** are non cytotoxic against MDA-MB-231, MCF-7 and A549 tumor cells. An enhancement of the cytotoxicity is observed in all cases when thiosemicarbazones and triphenylphosphine are coordinated to silver ion, most likely due to the higher cellular accumulation as a result of the increase of lipophilicity. In fact, cellular uptake results clearly indicated the internalization of silver complexes by the MDA-MB-231 cells, supporting the above conclusions. DNA binding studies have been carried out since the cytotoxic effect of metal complexes is frequently attributed to their ability to induce DNA damage, resulting in cell death.[51] Our results from DNA binding studies revealed that **1** displayed a poor DNA-binding affinity in cell free conditions, which may suggesting distinct pathways to cytotoxicity from that found for cisplatin. The cytotoxic effect of complex **1** on MDA-MB-231 cells was also evaluated under an inverted light microscope. Upon incubation with **1**, MDA-MB-231 cells exhibited the typical morphological changes associated with apoptosis: cell shrinkage and rounding together with their detachment from the plate.[36,37] Annexin V/ 7AAD flow cytometry analysis results confirm the apoptotic cell death in the MDA-MB-231 cells induced by compound **1**. In order to examine the changes that take place in cell cycle progression from inhibition of MDA-MB-231 cell proliferation, cell cycle distribution analysis using flow cytometry has been carried out. Upon incubation with complex **1**, an increase of the sub-G1 cell population with a concomitant accumulation in S-phase cells was noticed. The increase of the sub-G1 cell population indicates the induction of internucleosomal DNA fragmentation as a result of apoptosis].[39] In addition, complex **1** also induces S-phase cell cycle arrest, implying the inhibition of DNA synthesis or S-phase specific DNA damage.[52] Given its low reactivity towards ct-DNA, complex **1** may interfere with important enzymes in DNA replication, such as Topoisomerase I, a highly active enzyme during S-phase.[53] Another important difference between complex **1** and cisplatin can be noticed in their effects on mitochondrial membrane potential of MDA-MB-231 cells. Compound **1** induces a significant mitochondrial membrane depolarization in a concentration-dependent manner whilst cisplatin does not cause any effect under similar experimental conditions. These results suggest that complex **1** induces the apoptosis of MDA-MB-231 cells triggered by mitochondrial-dependent pathway.[54]

The ability of metal compounds to target mitochondria and induce the intrinsic (mitochondrial-dependent) apoptotic pathway has attracted considerable attention in the last few decades.[55–59] Much of this work has been focused on the role of gold compounds as "antimitochondrial agents".[59–62] Several mechanistic studies have demonstrated that the cytotoxic action of gold(I/III) compounds is linked with the inhibition of Thioredoxin reductases (TrxRs), a family of selenoproteins that take part in redox control of the mitochondrial permeability transition.[60,63–66] According to Bindoli et al.,[62] inhibition of mitochondrial and cytosolic TrxRs leads to an enhancement of $H_2O_2$ levels inside mitochondria and changes the permeability condition of the mitochondrial membranes, eventually leading to cell apoptosis.[62]

Besides gold-based compounds, silver(I) complexes have been identified to trigger apoptosis by targeting the mitochondria and/or inhibiting TrxRs.[55,63] The elegant Allison's work on the anti-cancer activity of $[Ag(NHC)_2][AgBr_2]$ (NHC = 1-benzyl-3-methylimidazolium) revealed that this compound is a powerful inhibitor of human TrxR ($IC_{50}$ value of 2.39 ± 0.59 nM), leading to an enhancement of ROS production and subsequently apoptotic cell death.[67] In addition, it induced the complete inhibition of Topoisomerase I at 0.16 μM, resulting in DNA damage together with the inhibition of PARP-1 and glycolysis in tumor cells.[67] A number of studies has also demonstrated the potential of silver(I) phosphine-based complexes to induce significant effects on mitochondria, which are associated with the mitochondriotropic properties of phosphines. For instance, triphenylphosphonium groups ($HPPh_3^+$/alkyl-$PPh_3^+$) have been used as vehicles to delivery drugs to mitochondria within because of their cationic charge and high lipophilicity.[37,55,68] Thus, the coordination of phosphines is supposed to play an important role in targeting mitochondria. For example, the complex $[Ag(SCN)(PR_3)]$ ($PR_3$ = tris(4-methoxyphenyl)phosphine) induces apoptosis via intrinsic pathway by the mitochondrial membrane depolarization, increase of ROS levels, caspase-9 cleavage and cytochrome c release.[17] Complexes of the type $[Ag(nim)(PR_3)_n]$ (nim = nimesulide; $PR_3$ = triarylphosphines; n = 1, 2) induces the apoptotic pathway in MCF-7 cells via mitochondrion damage.[37] In addition, these silver phosphine complexes showed inhibitory activity against the lipoxygenase (LOX), an enzyme mainly distributed to mitochondrion and responsible for the oxidation of polyunsaturated fatty acids to leukotrienes or prostaglandins.[37]

However, reports on TrxR inhibition by silver phosphine compounds are still scarce in literature. According to Santini *et al.*,[69] the cytotoxic activity of $[Ag(PTA)_4]PF_6$ (PTA = 1,3,5-triaza-7-phosphaadamantane) against tumour cells has been proposed to be the result of its ability to inhibit cytosolic TrxR ($IC_{50}$ value of 10.3 nM). Recently, Landini *et al.* have reported the cytotoxicity and TrxR inhibition studies on complexes of the type $[MX(PEt_3)]$ and $[M(PEt_3)_2]^+$ (M = Ag, Au; X = halides; $PEt_3$= triethylphosphine).[70] Although silver complexes have elicited the TrxR inhibition at $IC_{50}$ values ranging from 11-49 nM, they were less potent than their corresponding gold analogues. According to the authors, the moderate effect induced by silver compounds in the TrxR activity in treated cells compared to that of gold species suggests that additional mechanism of cell damage may be involved.

Based on the results of the studies discussed above, we suggest that mitochondria may be one of the cellular targets responsible for the cytotoxic effects of **1** in the MDA-MB-231 cells rather than DNA. However, further studies are required to evidence if these silver species or their products of biological reactions are able to reach nucleus so that DNA binding may be significant to the cytotoxicity. At this point, the mechanisms of action associated with its mitochondrial pathway remain to be elucidated. Although we cannot confirm that **1** induces ROS production, its interaction with Thioredoxin reductases and other proteins cannot be discarded.

View Article Online
DOI: 10.1039/D0DT01134G



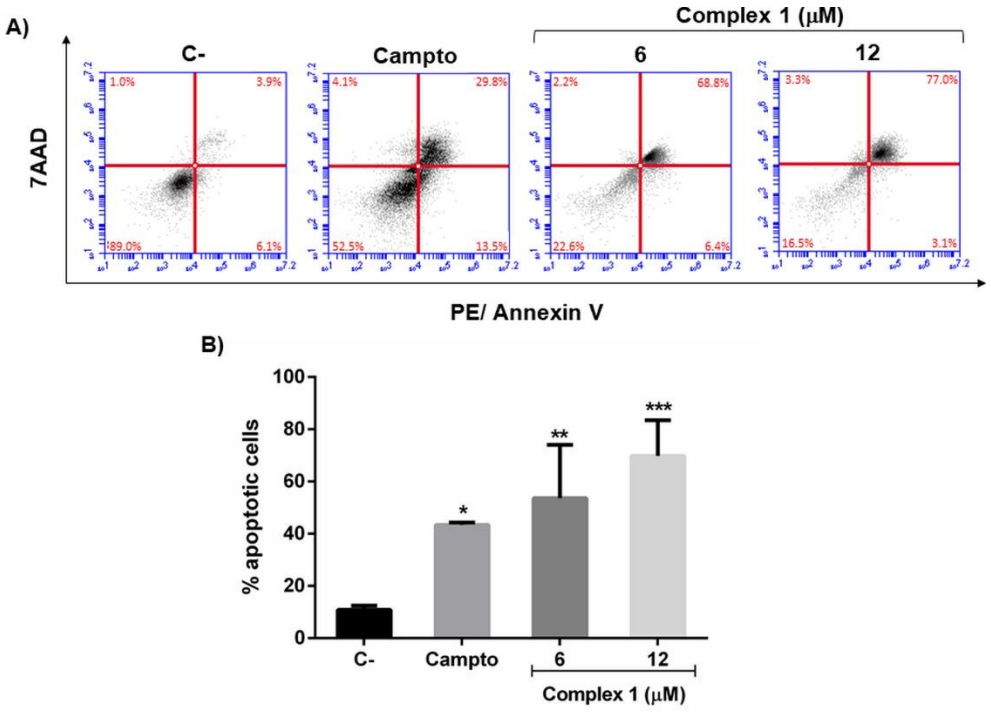


**Fig. 4** A) Complex **1** induce apoptosis in TNBC cells. MDA-MB-231 cells were exposed to **1** and analyzed by flow cytometry. B) Percentage of apoptotic cells compared to the control cells. The percentage of cells in apoptosis was calculated as the sum of the cells in recent and late apoptosis. Camptothecin (Campto, 20 μM) was used as positive control. A representative dot plot for each condition is shown. Data are the mean of experiments in triplicate (*p ≤ 0.05, **p ≤ 0.01 and ***p ≤ 0.001).

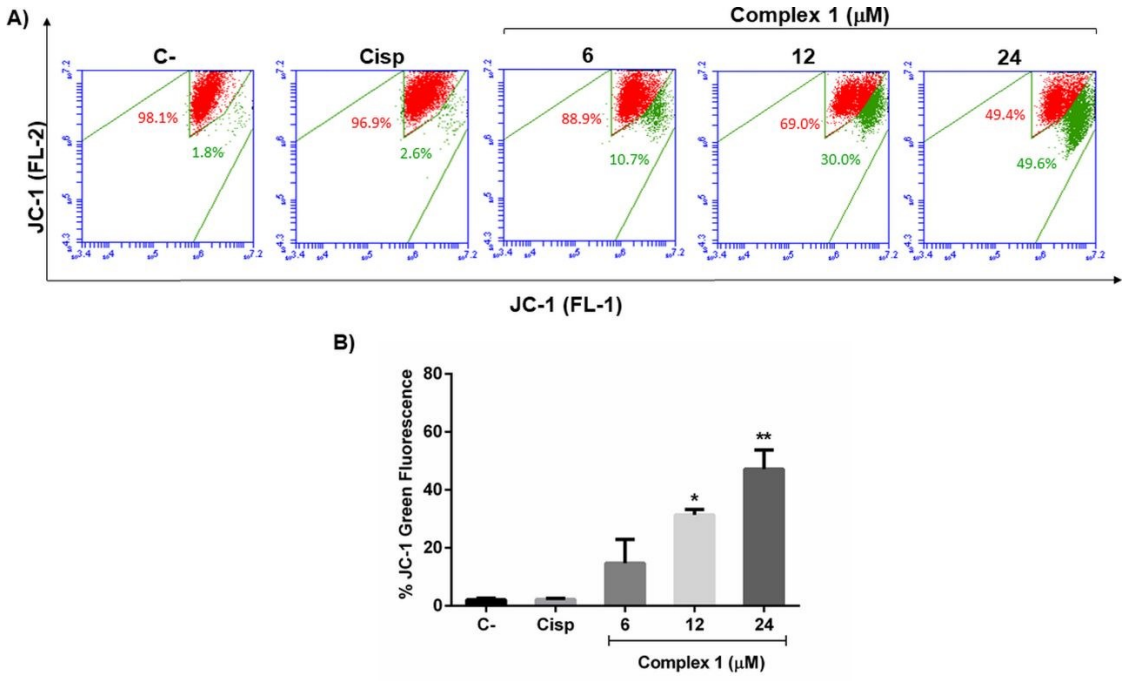


**Fig. 5** A) Effects of complex **1** on mitochondrial membrane potential (Δψm) of MDA-MB-231 cells. Cells with normal mitochondrial membranes are exhibited in red, whereas cells with loss of Δψm are depicted in green. TNBC cells were incubated with **1** (6, 12 and 24 μM) or 50 μM of cisplatin

(Cisp) for 4 h, and stained with JC-1. B) Percentage of cells emitting green fluorescence. A representative dot plot for each condition is shown. Data are the mean of experiments in triplicate (*p ≤ 0.001 and **p ≤ 0.0001).

View Article Online
DOI: 10.1039/D0DT01134G

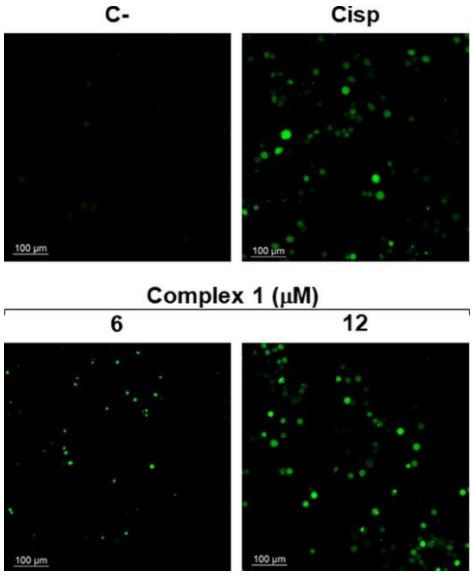


**Fig. 6** Effects of complex **1** on intracellular ROS formation in MDA-MB-231 cells. TNBC cells were incubated with **1** (6 and 12 μM) or 50 μM of cisplatin (Cisp) for 24 h, and stained with $H_2$DCFDA.

## Conclusions

In this work, we have synthesized new tetrahedral silver(I) compounds of the type $[AgCl(PPh_3)_2(L)]$ {$PPh_3$ = triphenylphosphine; L= **VTSC** = 3-methoxy-4-hydroxybenzaldehyde thiosemicarbazone (**1**); **VMTSC** = 3-methoxy-4-[2-(morpholine-1-yl)ethoxy)benzaldehyde thiosemicarbazones (**2**); **VPTSC** = 3-methoxy-4-[2-(piperidine-1-yl)ethoxy)benzaldehyde thiosemicarbazone (**3**)} and evaluated their cytotoxic and apoptotic effects. The molecular structures of **2** and **3** have been confirmed by single crystal X-ray diffraction studies. The new vanillin thiosemicarbazones **VMTSC** and **VPTSC** were inactive against human tumor breast (MDA-MB-231 and MCF-7) and lung (A549) cells. The new silver compounds are more potent than cisplatin against all tested tumour cells. In general, silver complexes **1**-**3** showed comparable cytotoxicity, indicating that the incorporation of *O*-alkylated vanillin thiosemicarbazones did not result in an increased cytotoxicity. After 3 hours of incubation, ca. 30% of **1**-**3** were internalized in MDA-MB-231 cells, which suggest that a significant amount of the complexes reach the cell's interior. Compound **1** induced apoptosis and mitochondrial membrane depolarization. DNA binding studies confirm that **1** can interact with DNA (and will do so via a mechanism different to that of cisplatin) though it does so weakly which implies that other targets in the cell may be equally or more important. Although the exact pharmacological targets associated with the cytotoxicity of **1** remain unclear, our evidences indicated mitochondria as a potential intracellular targets for these silver compounds rather than DNA. The mechanisms of action involved with its antimitochondrial activity are still unknown but the interaction with enzymatic targets, such as Thioredoxin reductases, cannot be ruled out. These findings demonstrated that silver compounds could be potentially useful for the development of new metal-based drugs to treat triple negative breast cancer proliferation.

## Experimental section

### Chemistry

Silver chloride and organic reagents were purchased from Sigma. Literature procedures were followed for the synthesis of 3-methoxy-4-hydroxybenzaldehyde thiosemicarbazone (VTSC)[71] and the functionalized aldehydes (3-methoxy-4-[2-(piperidine-1-yl)ethoxy)benzaldehyde (VP) and 3-methoxy-4-[2-(morpholine-1-yl)ethoxy)benzaldehyde (VM).[24] The silver(I) complexes were synthetized under protection of light. Elemental analyses data were obtained with a Perkin Elmer 2400 series II. IR spectra were recorded on a Perkin Elmer Spectrum 200 spectrometer in the range of 4000–400 $cm^{-1}$ using KBr pellets. The $^1$H and DEPTQ NMR spectra were recorded on a 14.1 T Bruker Avance III HD spectrometer at 298 K.

### Crystal structure determination

Single crystal X-ray diffraction data for both complexes were collected at room temperature (293 K) on a Rigaku XTALAB-MINI diffractometer using MoKα radiation (0.71073 Å) monochromated by graphite. The cell determination and the final cell parameters were obtained on all reflections using the software *CrysAlisPro*.[72] Data integration and scaled was carried out using the software *CrysAlisPro*. The structures were solved by direct method using SHELXT[73] and refined using full-matrix least-squares method within SHELXL software,[74] included in Olex2.[75] In all cases, non-hydrogen atoms were clearly resolved in the Fourier maps and anisotropically refined. Hydrogen atoms were stereochemically positioned and refined using the riding model.[74] The crystallographic data are summarized in Table 1. The crystallographic illustrations were prepared MERCURY program.[76] The CIF file of structures **2** and **3** were deposited in the Cambridge Structural Data Base under the code CCDC 1992316 and 1992321, respectively. Copies of the data can be obtained, free of charge, via www.ccdc.cam.ac.uk.

### Synthesis

### Thiosemicarbazones

*3-methoxy-4-hydroxybenzaldehyde thiosemicarbazone* **(VTSC)** Yield 81%. IR (KBr, $cm^{-1}$): 3170 ν(NH); 1598 ν(C=N); 758 ν(C=S). $^1$H NMR (DMSO-$d_6$, δ ppm): 11.26 (s, 1H, =N-NH-), 9.49 (s, 1H, OH), 8.11 and 7.96 (s, 2H, $NH_2$), 7.93 (s, 1H, HC=N), 7.47 (d, J = 1.75 Hz, 1H, H2van), 7.02 (dd, J = 8.20, 1.85 Hz, 1H, H6van), 6.78 (d, J = 8.20 Hz, 1H, H5van), 3.82 (s, 3H, $OCH_3$). DEPTQ NMR (DMSO-$d_6$, δ ppm): 177.38 (C=S), 148.84 (C4), 148.14 (C3),

142.97 (HC=N), 125.64 (C1), 122.44 (C6), 115.24 (C5), 109.27 (C2), 55.81 ($OCH_3$).

*3-methoxy-4-[2-(4-morpholine-1-yl)ethoxy]-benzaldehyde thiosemicarbazone* **(VMTSC)**

A round bottom flask was charged with 3-methoxy-4-[2-(morpholine-1-yl)ethoxy)benzaldehyde (2.24 mmols), thiosemicarbazide (2.24 mmols) and 20 mL of ethanol aqueous solution ($V_{water}$ :$V_{ethanol}$ = 3:1). After the addition of a catalytic amount of diluted HCl, the reaction mixture was kept under magnetic stirring at room temperature. After 24 h, the pH of the reaction media was adjusted to 9 by adding $K_2CO_3$, affording a microcrystalline solid. The solid was filtered off, washed carefully with ice water and cool MeOH, and dried under vacuum. Yield: 72 %. Anal. Calc. for C15H28N4O6S (%): C, 45.90; H, 7.19; N, 14.28. Found (%): C, 45.87; H, 6.88; N, 14.17. IR (KBr, $cm^{-1}$): 3170 ν(NH); 1600 ν(C=N); 766 ν(C=S). $^1$H NMR (DMSO-$d_6$, δ ppm): 11.31 (s, 1H, =N-NH-), 8.16 and 8.02 (s, 2H, $NH_2$), 7.96 (s, 1H, HC=N), 7.51 (d, J=1.85 Hz, 1H, H2van), 7.11 (dd, J= 8.40, 1.85 Hz, 1H, H6van), 6.99 (d, J=8.40 Hz, 1H, H5van), 4.09 (t, J= 6.0 Hz, 2H, $O\underline{CH_2}CH_2N$), 3.81 (s, 3H, $OCH_3$), 3.57 (t, J= 4.5 Hz, 4H, H1morf), 2.69 (t, J=5.7 Hz, 2H, $OCH_2\underline{CH_2}N$), 2.48 (b, 4H, H2morf). DEPTQ NMR (DMSO-$d_6$, δ ppm): 177.53 (C=S), 149.80 (C4), 149.32 (C3), 142.52 (HC=N), 127.10 (C1), 122.17 (C6), 112.53 (C5), 108.79 (C2), 66.19 (C1morf), 66.13 ($OCH_2\underline{CH_2}N$), 56.98 ($O\underline{CH_2}CH_2N$), 55.80 ($OCH_3$), 53.71 (C2morf).

*3-methoxy-4-[2-(4-piperidine-1-yl)ethoxy]-benzaldehyde thiosemicarbazone* **(VPTSC)**

The preparation was the same as that of **VMTSC**, except that 3-methoxy-4-[2-(piperidine-1-yl)ethoxy)benzaldehyde (**VP**) was used. Yield: 83 %. Anal. Calc. for C16H30N4O5S (%): C, 49.21; H, 7.74; N,14.35. Found (%): C, 49.05; H, 7.77; N, 14.14. IR (KBr, $cm^{-1}$): 3170 ν(NH); 1600 ν(C=N); 780 ν(C=S). $^1$H NMR (DMSO-$d_6$, δ ppm): 11.31 (s, 1H, =N-NH-), 8.15 and 8.02 (s, 2H, $NH_2$), 7.95 (s, 1H, HC=N), 7.51 (d, J= 1.85 Hz, 1H, H2van), 7.11 (dd, J= 1.85, 8.40 Hz, 1H, H6van), 6.98 (d, J= 8.40 Hz, 1H, H5van), 4.07 (t, J= 6 Hz, 2H, $O\underline{CH_2}CH_2N$), 3.81 (s, 3H, $OCH_3$), 2.65 (t, J= 6 Hz, 2H, $OCH_2\underline{CH_2}N$), 2.43 (b, 4H, H1pip), 1.48 (q, J= 6 Hz, 4H, H2pip), 1.36 (b, 2H, H3pip). DEPTQ NMR (DMSO-$d_6$, δ ppm): 177.51 (C=S), 149.85 (C4), 149.28 (C3), 142.53 (HC=N), 127.01 (C1), 122.18 (C6), 112.47 (C5), 108.77 (C2), 66.31 ($OCH_2\underline{CH_2}N$), 57.32 ($O\underline{CH_2}CH_2N$), 55.78 ($OCH_3$), 54.48 (C1pip), 25.57 (C2pip), 23.93 (C3pip).

**Silver(I) compounds**

*[AgCl($PPh_3$)$_2$(VTSC)]* **(1)**

3-methoxy-4-hydroxybenzaldehyde thiosemicarbazone (80 mg, 0.355 mmol) was added to a suspension of AgCl (50.89 mg, 0.355 mmol) in 10 mL of acetonitrile and stirring for 24 hours at 50 °C. After this period, triphenylphosphine (186.28 mg, 0.71 mmol) was added and stirred for 30 minutes leading to a clear solution. The solution was kept to crystallization at room temperature. Yield: 40%. Anal. Calc. for C45H41AgClN3O2P2S (%): C, 60.51; H, 4.63; N, 4.70. Found (%): C, 59.94; H, 4.77; N, 4.69. IR (KBr, $cm^{-1}$): 1598 ν(C=N); 1095 ν(P-CPh); 745 ν (C=S). $^1$H NMR (DMSO-$d_6$, δ ppm): 11.62 (s, 1H, =N-NH-), 9.53 (s, 1H, OH), 8.48 and 8.19 (s, 2H, $NH_2$), 8.00 (s, 1H, HC=N), 7.50 (d, J = 1.75 Hz, 1H, H2van), 7.44 (m, 6H, $PPh_3$), 7.34 (m, 24H, $PPh_3$), 7.04 (dd, J = 8.0, 1.75 Hz, 1H, H6van), 6.79 (d, J = 8.0 Hz, 1H, H5van), 3.83 (s, 3H, $OCH_3$). $^{13}$C NMR (DMSO-$d_6$, δ ppm): 175.97 (C=S), 149.06 (C4), 148.15 (C3), 144.15 (HC=N), 133.57 (CH $PPh_3$), 133.20 (Cq $PPh_3$), 130.13 (CH $PPh_3$), 128.91 (CH $PPh_3$), 125.37 (C1), 122.68 (C6), 115.23 (C5), 109.34 (C2), 55.79 ($OCH_3$).

The compounds **2** and **3** were prepared similarly to **1**.

*[AgCl($PPh_3$)$_2$(VMTSC)]* **(2)**

Yield 48%. Anal. Calc. for C51H52AgClN4O3P2S (%): C, 60.87; H, 5.21; N, 5.57. Found (%): C, 58.08; H, 5.20; N, 5.38. IR (KBr, $cm^{-1}$): 1600 ν(C=N); 1095 ν(P-CPh); 745 ν (C=S). $^1$H NMR (DMSO-$d_6$, δ ppm): 11.60 (s, 1H, =N-NH-), 8.44 and 8.19 (s, 2H, $NH_2$), 8.01 (s, 1H, HC=N), 7.53 (d, J=1.75 Hz, 1H, H2van), 7.45 (m, 6H, $PPh_3$), 7.36 (m, 24H, $PPh_3$), 7.13 (dd, 8.40, 1.75 Hz, 1H, H6van) 6.99 (d, J= 8.40 Hz, 1H, H5van), 4.10 (t, J= 6.0 Hz, 2H, $OCH_2CH_2N$), 3.82 (s, 3H, $OCH_3$), 3.57 (t, J= 4.5 Hz, 4H, H1morf), 2.69 (t, J=5.7 Hz, 2H, $OCH_2CH_2N$), 2.47 (b, 2H, H2morf). $^{13}$C NMR (DMSO-$d_6$, δ ppm): 176.40 (C=S), 149.95 (C4), 149.30 (C3), 143.50 (HC=N), 133.41 (CH $PPh_3$), 133.28 (Cq $PPh_3$), 130.07 (CH $PPh_3$), 128.84 (CH $PPh_3$), 126.87 (C1), 122.32 (C6), 112.53 (C5), 108.88 (C2), 66.19 (C1morf), 66.17 ($OCH_2CH_2N$), 56.95 ($OCH_2CH_2N$), 55.78 ($OCH_3$), 53.68 (C2morf).

*[AgCl($PPh_3$)$_2$(VPTSC)]* **(3)**

Yield 53%. Anal. Calc. for C54H57AgClN5O2P2S (%): C, 62.04; H, 5.50; N, 6.70. Found (%): C, 61.92; H, 5.48; N, 6.54. IR (KBr, $cm^{-1}$): 1600 ν(C=N); 1095 ν(P-CPh); 745 ν (C=S).$^1$H NMR (DMSO-$d_6$, δ ppm): 11.73 (s, 1H, =N-NH-), 8.54 and 8.26 (s, 2H, $NH_2$), 8.03 (s, 1H, HC=N), 7.53 (d, J= 1.85 Hz, 1H, H2van), 7.43 (m, 6H, $PPh_3$), 7.33 (m, 24H, $PPh_3$), 7.13 (dd, J= 1.85, 8.35 Hz, 1H, H6van), 7.00 (d, J= 8.40 Hz, 1H, H5van), 4.08(t, J= 6 Hz, 2H, $OCH_2CH_2N$), 3.82 (s, 3H, $OCH_3$), 2.66(t, J= 6 Hz, 2H, $OCH_2CH_2N$), 2.44 (b, 4H, H1pip), 1.49 (q, J= 6 Hz, 4H, H2pip), 1.37 (b, 2H, H3pip). $^{13}$C NMR (DMSO-$d_6$, δ ppm): 176.03 (C=S), 150.03 (C4), 149.28 (C3), 143.79 (HC=N), 133.44 (CH $PPh_3$), 133.16 (Cq $PPh_3$), 130.10 (CH $PPh_3$), 128.81 (CH $PPh_3$), 126.76 (C1), 122.42 (C6), 112.43 (C5), 108.82 (C2), 66.30 ($OCH_2CH_2N$), 57.31 ($OCH_2CH_2N$), 55.77 ($OCH_3$), 54.46 (C1pip), 25.56 (C2pip), 23.92 (C3pip).

**Stability studies**

The $^1$H NMR spectra of compounds **1-3** in DMSO-$d_6$/$D_2O$ (80: 20% v/v) were acquired on a 14.1 T Bruker Avance III HD spectrometer at 0, 24 and 48 h after preparation of samples (298 K).

The UV-VIS spectra of compound **1-3** ($2x10^{-5}$ mol $L^{-1}$) prepared in Tris-HCl buffer (5 mM Tris-HCl and 50 mM NaCl, pH 7.4) with 2% DMSO were recorded at 0, 24 and 48 h after preparation of solutions.

**Cell culture.** The human lung tumor cell line A549 was obtained from ATCC, and human breast tumor cell lines MCF-7 and MDA-MB-231 were from Rio de Janeiro Cell Bank (BCRJ). The cells were maintained at 37 °C in 5% $CO_2$ in Dulbecco's Modified

Eagle´s medium (DMEM), supplemented with 10% of FBS, gentamicin sulfate (50 mg $L^{-1}$) and amphotericin B (2 mg $L^{-1}$). The non-tumor cells MCF-10A (breast) were obtained from Olivia Newton-John Institute Cancer Research Institute, maintained at 37 °C in 5% $CO_2$ in Dulbecco's Modified Eagle´s Medium and Nutrient Mixture F-12 (DMEM/ F12), supplemented with 5% horse serum, EGF (0.02 mg $mL^{-1}$), hydrocortisone (0.05 mg $mL^{-1}$), insulin (0.01 mg $mL^{-1}$), L- glutamine (2 mM), penicillin (100 UI $mL^{-1}$) and streptomycin (100 mg $mL^{-1}$).

**Cell viability.** The cytotoxic effects of compounds were determined by MTT [3-(4,5-dimethylthiazol-2-yl)-2,5-diphenyltetrazolium bromide] assay. The cells ($1.5x10^4$ cells/ 100μL) were seeded in 96-well plates and incubated at 37 °C in 5% $CO_2$ for 24 h. Then, the cells were treated with different concentrations of compounds for 48 h. The silver compounds and ligands were solubilized in DMSO, whereas cisplatin was prepared in DMF. The control cells were incubated with 0.5% of DMSO (vehicle). After treatment, the medium was removed and the cells were incubated with MTT (1 mg $mL^{-1}$) for 4 h. Next, the formazan crystals were solubilized in isopropanol and absorbance measured on a micro plate reader (BioTek, Epoch) at 570 nm. The $IC_{50}$ values were calculated using the Hill's equation in the Graph Pad Prism software 6.0.

**Cellular uptake.** MDA-MB-231 cells ($2x10^5$ cells per well) were seeded in 12-well plates and incubated at 37 °C in 5% $CO_2$. After 24 h, the cells were treated with 12 μM of compounds **1-3** for 3 h. Then, the medium was removed and cells were washed with PBS (phosphate buffered saline), trypsinized and the cell suspension counted. The total concentration of Ag was determined using an Analytik Jena ContrAA 700 high-resolution continuum source graphite furnace atomic absorption spectrometer. Analytical working solution containing 50 μg $L^{-1}$ Ag was prepared daily by dilution of the 1000 mg $L^{-1}$ stock standard solution (SpecSol®, QUIMLAB, Brazil) and acidified to 1.0% (v/v) $HNO_3$ solution. The blank solution was 1.0 % (v/v) $HNO_3$. External calibration was adopted. The calibration curve was performed by addition of appropriate aliquots of analytical working solution into the atomizer in order to obtain 50, 100, 150, 250, 350, 500 and 750 pg of Ag. The samples consisting in cell suspension with internalized compounds **1-3** were diluted in deionized water and homogenized on a vortex mixer and aliquots of 5 μL analyzed. Each sample was read in triplicate. To consider the matrix effects, the concentration of Ag was also determined in samples with initial concentration of **1-3** (12 μM). The results are expressed as percentage of Ag uptake (See ESI).

**Morphology assay.** The MDA-MB-231 cells ($0.4x10^5$ cells per well) were seeded in 24-well plates, incubated at 37 °C in 5% $CO_2$ for 24 h and then, exposed to 6, 12 and 24 μM of compound **1** for 48 h. Cell morphology was examined under an inverted microscope (LABOMED TCM 400) and the images were recorded using a camera (LABOMED iVu5100).

**Apoptosis assay.** The Annexin V/ 7-AAD double staining assay was performed to analyze the effects of compound **1** on apoptosis. The MDA-MB-231 cells ($0.4x10^5$ cells per well) were seeded in 24-well plates and maintained at 37 °C in 5% $CO_2$ for 24 h and then, treated with 6 and 12 μM of **1** for 48 h. The cells were washed with PBS and incubated with 2.5 μL de 7AAD and 2.5 μL PE-Annexin-V (BD Biosciences) for 15 min. Next, the cells were collected with a scraper and analyzed in an Accuri C6 flow cytometer (BD Biosciences) using the CSampler software (BD Biosciences).

**Cell cycle assay.** MDA-MB-231 cells ($1x10^5$ cells per well) were seeded in 12-well plates and incubated at 37 °C in 5% $CO_2$ for 24 h. After incubation, the cells were treated with 6 μM of **1** for 48 h. Then, the cells were harvested and fixed with 70% ethanol at -20 °C for 24 h, washed with PBS and incubated with a solution containing 0.02 μg $mL^{-1}$ RNase A (Sigma) and 10 μg $mL^{-1}$ PI (Sigma) at 37 °C for 30 min. Next, the cells were analyzed in an Accuri C6 flow cytometer (BD Biosciences) using the CSampler software (BD Biosciences).

**The mitochondrial membrane potential (Δψm) assay**. Flow cytometry assays using the BD MitoScreen kit (BD Biosciences) were performed to investigate the effects of compound **1** in the mitochondrial Δψm. MDA-MB-231 cells ($1x10^5$ cells per well) were seeded in 12-well plates, incubated at 37 °C in 5% $CO_2$ for 24 h and then, treated with 6, 12 and 24 μM of **1** for 4 h. The cells were harvested and incubated with 10 μg $mL^{-1}$ of JC-1 (5,5′,6,6′-Tetrachloro-1,1′,3,3′-tetraethyl-imidacarbocyanine iodide) at 37 °C for 15 min. Next, the cells were washed with PBS and analyzed in an Accuri C6 flow cytometer (BD Biosciences) using CSampler software (BD Biosciences).

**ROS assay.** MDA-MB-231 cells ($0.4x10^5$ cells per well) were seeded in 24-well plates, incubated at 37 °C in 5% $CO_2$ for 24 h and then, exposed to 6 and 12 μM of **1** for 24 h. The cells were washed with PBS and incubated with 10 μM of $H_2$DCFDA (2',7'-dichlorodihydrofluorescein diacetate, Invitrogen) at 37 °C for 20 min. Then, the cells were analyzed using a confocal fluorescence microscope (Carl Zeiss LSM 800).

**DNA binding assays**

All experiments were carried out from a fresh solution of ct-DNA (Sigma) prepared in Tris-HCl buffer (5 mM Tris-HCl and 50 mM NaCl, pH 7.4). The compound **1** solution was initially prepared in DMSO and then diluted to different concentrations in Tris-HCl buffer, with the DMSO concentration kept below 3%.

The CD spectra were recorded on a spectropolarimeter JASCO J-815 in a continuous mode scanning (100 nm $min^{-1}$) with accumulations of 4 scans, from 235 to 300 nm. The spectra were obtained for free ct-DNA (50 μM) and in the presence of different concentrations of **1** (from 2.5 to 15 μM). The samples were incubated for 24 h at 37 °C.

The competitive binding studies were performed in a JASCO J-815 equipped with fluorescence detector. The DNA and Hoechst 33258 concentrations were kept fixed at 60 μM and 6 μM, respectively, while the concentration of the compound **1** range from 0 to 60 μM. The samples were maintained in rest for

5 min before the measurements and then, the spectra were obtained from 360 to 600 nm with excitation wavelength at 350 nm.

## Conflicts of interest

The authors declare that they have no conflict of interest.

## Acknowledgements

The authors are grateful for the financial support provided by FAPESP (proc. 2013/26203-5, 2015/12098 and 2016/177115), CNPq (proc. 422105/2016-3, 407676/2016-3 and 305190/2017-2) and CAPES.

## Notes and references

1 F. Bray, J. Ferlay, I. Soerjomataram, R. L. Siegel, L. A. Torre and A. Jemal, *CA. Cancer J. Clin.*, 2018, **68**, 394–424.

2 A. Toss and M. Cristofanilli, *Breast Cancer Res.*, 2015, **17**, 1–11.

3 J. D. C. Hon, B. Singh, A. Sahin, G. Du, J. Wang, V. Y. Wang, F. M. Deng, D. Y. Zhang, M. E. Monaco and P. Lee, *Am. J. Cancer Res.*, 2016, **6**, 1864–1872.

4 C. N. Banti and S. K. Hadjikakou, *Metallomics*, 2013, **5**, 569–596.

5 S. Medici, M. Peana, G. Crisponi, V. M. Nurchi, J. I. Lachowicz, M. Remelli and M. A. Zoroddu, *Coord. Chem. Rev.*, 2016, **327–328**, 349–359.

6 S. Medici, M. Peana, V. M. Nurchi and M. A. Zoroddu, *J. Med. Chem.*, 2019, **62**, 5923–5943.

7 X. Liang, S. Luan, Z. Yin, M. He, C. He, L. Yin, Y. Zou, Z. Yuan, L. Li, X. Song, C. Lv and W. Zhang, *Eur. J. Med. Chem.*, 2018, **157**, 62–80.

8 S. J. Berners-Price and P. J. Sadler, *Bioinorg. Chem. Struct. Bond.*, 1988, 27–102.

9 F. J. Ramos-Lima, A. G. Quiroga, B. García-Serrelde, F. Blanco, A. Carnero and C. Navarro-Ranninger, *J. Med. Chem.*, 2007, **50**, 2194–2199.

10 S. J. Berners-Price, R. K. Johnson, A. J. Giovenella, L. F. Faucette, C. K. Mirabelli and P. J. Sadler, *J. Inorg. Biochem.*, 1988, **33**, 285–295.

11 S. Zartilas, S. K. Hadjikakou, N. Hadjiliadis, N. Kourkoumelis, L. Kyros, M. Kubicki, M. Baril, I. S. Butler, S. Karkabounas and J. Balzarini, *Inorganica Chim. Acta*, 2009, **362**, 1003–1010.

12 Z. Human-Engelbrecht, R. Meijboom and M. J. Cronjé, *Cytotechnology*, 2017, **69**, 591–600.

13 Z. Human, A. Munyaneza, B. Omondi, N. M. Sanabria, R. Meijboom and M. J. Cronjé, *BioMetals*, 2015, **28**, 219–228.

14 S. K. Hadjikakou, L. Kyros, N. Kourkoumelis, M. Kubicki, L. Male, M. B. Hursthouse, I. I. Verginadis, E. Gouma, S. Karkabounas and K. Charalabopoulos, *Bioinorg. Chem. Appl.*, 2010, **2010**, 386860.

15 K. Potgieter, Z. Engelbrecht, G. Naganagowda, M. J. Cronjé and R. Meijboom, *J. Coord. Chem.*, 2017, **70**, 2644–2658.

16 M. Poyraz, C. N. Banti, N. Kourkoumelis, V. Dokorou, M. J. Manos, M. Simčič, S. Golič-Grdadolnik, T. Mavromoustakos, A. D. Giannoulis, I. I. Verginadis, K. Charalabopoulos and S. K. Hadjikakou, *Inorganica Chim. Acta*, 2011, **375**, 114–121.

17 Z. Engelbrecht, R. Meijboom and M. J. Cronjé, *BioMetals*, 2018, **31**, 189–202.

18 D. E. S. Silva, A. B. Becceneri, M. C. Solcia, J. V. B. Santiago, M. B. Moreira, J. A. Gomes Neto, F. R. Pavan, M. R. Cominetti, J. C. M. Pereira and A. V. G. Netto, *Dalt. Trans.*, 2020, **49**, 5264–5275.

19 F. Bisceglie, M. Tavone, F. Mussi, S. Azzoni, S. Montalbano, S. Franzoni, P. Tarasconi, A. Buschini and G. Pelosi, *J. Inorg. Biochem.*, 2018, **179**, 60–70.

20 G. A. da Cunha, R. F. F. de Souza, R. L. de Farias, M. B. Moreira, D. E. S. Silva, R. D. Zanetti, D. M. Garcia, D. G. Spindola, L. F. G. Michelin, C. Bincoletto, A. A. de Souza, A. A. Antunes, W. A. d. S. Judice, R. C. F. Leitao, V. M. Deflon, A. E. Mauro and A. V. G. Netto, *J. Inorg. Biochem.*, 2020, **203**, 110944.

21 P. F. Espuri, L. L. dos Reis, E. de Figueiredo Peloso, V. S. Gontijo, F. A. Colombo, J. B. Nunes, C. E. de Oliveira, E. T. De Almeida, D. E. S. Silva, J. Bortoletto, D. F. Segura, A. V. G. Netto and M. J. Marques, *J. Biol. Inorg. Chem.*, 2019, **24**, 419–432.

22 R. F. F. de Souza, G. A. da Cunha, J. C. M. Pereira, D. M. Garcia, C. Bincoletto, R. N. Goto, A. M. Leopoldino, I. C. da Silva, F. R. Pavan, V. M. Deflon, E. T. de Almeida, A. E. Mauro and A. V. G. Netto, *Inorganica Chim. Acta*, 2019, **486**, 617–624.

23 F. V. Rocha, R. L. Farias, M. A. Lima, V. S. Batista, N. M. Nascimento-Júnior, S. S. Garrido, A. M. Leopoldino, R. N. Goto, A. B. Oliveira, J. Beck, C. Landvogt, A. E. Mauro and A. V. G. Netto, *J. Inorg. Biochem.*, 2019, **199**, 110725.

24 Y. Pourshojaei, A. Abiri, K. Eskandari, Z. Haghighijoo, N. Edraki and A. Asadipour, *Sci. Rep.*, 2019, **9**, 19855.

25 T. S. Lobana, R. Sharma, G. Bawa and S. Khanna, *Coord. Chem. Rev.*, 2009, **253**, 977–1055.

26 T. S. Lobana, R. Sharma and R. J. Butcher, *Polyhedron*, 2009, **28**, 1103–1110.

27 T. S. Lobana, S. Khanna, R. Sharma, G. Hundal, R. Sultana, M. Chaudhary, R. J. Butcher and A. Castineiras, *Cryst. Growth Des.*, 2008, **8**, 1203–1212.

28 A. Khan, J. P. Jasinski, V. A. Smolenski, E. P. Hotchkiss, P. T. Kelley, Z. A. Shalit, M. Kaur, K. Paul and R. Sharma, *Bioorg. Chem.*, 2018, **80**, 303–318.

29 D. F. Segura, A. V. G. Netto, R. C. G. Frem, A. E. Mauro, P. B. Da Silva, J. A. Fernandes, F. A. A. Paz, A. L. T. Dias, N. C. Silva, E. T. De Almeida, M. J. Marques, L. De Almeida, K. F. Alves, F. R. Pavan, P. C. De Souza, H. B. De Barros and C. Q. F. Leite, *Polyhedron*, 2014, **79**, 197–206.

30 W. McFarlane, P. D. Akrivos, P. Aslanidis, P. Karagiannidis, C. Hatzisymeon, M. Numan and S. Kokkou, *Inorganica Chim. Acta*, 1998, **281**, 121–125.

31 P. Papathanasiou, G. Salem, P. Waring and A. C. Willis, *J.*

*Chem. Soc., Dalt. Trans.*, 1997, 3435–3443.
32 S. J. Berners-Price, P. J. Sadler and C. Brevard, *Magn. Reson. Chem.*, 1990, **28**, 145–148.
33 D. Gerlier and N. Thomasset, *J. Immunol. Methods*, 1986, **94**, 57–63.
34 H. Scheffler, Y. You and I. Ott, *Polyhedron*, 2010, **29**, 66–69.
35 T. S. Reddy, S. H. Privér, N. Mirzadeh and S. K. Bhargava, *Eur. J. Med. Chem.*, 2018, **145**, 291–301.
36 C. N. Banti, A. D. Giannoulis, N. Kourkoumelis, A. M. Owczarzak, M. Kubicki and S. K. Hadjikakou, *Dalt. Trans.*, 2014, **43**, 6848–6863.
37 C. N. Banti, C. Papatriantafyllopoulou, M. Manoli, A. J. Tasiopoulos and S. K. Hadjikakou, *Inorg. Chem.*, 2016, **55**, 8681–8696.
38 P. Yu, C. Zhang, C.-Y. Gao, T. Ma, H. Zhang, M.-M. Zhou, Y.-W. Yang, L. Yang and L.-Y. Kong, *Oncotarget*, 2017, **8**, 64032–64049.
39 X. Huang, H. D. Halicka, F. Traganos, T. Tanaka, A. Kurose and Z. Darzynkiewicz, *Cell Prolif.*, 2005, **38**, 223–243.
40 Z. Darzynkiewicz, S. Bruno, G. Del Bino, W. Gorczyca, M. A. Hotz, P. Lassota and F. Traganos, *Cytometry*, 1992, **13**, 795–808.
41 E. Robles-Escajeda, D. Lerma, A. M. Nyakeriga, J. A. Ross, R. A. Kirken, R. J. Aguilera and A. Varela-Ramirez, *PLoS One*, 2013, **8**, e73508.
42 D. Trachootham, J. Alexandre and P. Huang, *Nat. Rev. Drug Discov.*, 2009, **8**, 579–591.
43 C. H. Ng, S. M. Kong, Y. L. Tiong, M. J. Maah, N. Sukram, M. Ahmad and A. S. B. Khoo, *Metallomics*, 2014, **6**, 892–906.
44 V. T. Yilmaz, C. Icsel, F. Suyunova, M. Aygun, B. Cevatemre and E. Ulukaya, *New J. Chem.*, 2017, **41**, 8092–8106.
45 W. Cao, J. Qi, K. Qian, L. Tian, Z. Cheng and Y. Wang, *J. Inorg. Biochem.*, 2019, **191**, 174–182.
46 B. Kalyanaraman, V. Darley-Usmar, K. J. A. Davies, P. A. Dennery, H. J. Forman, M. B. Grisham, G. E. Mann, K. Moore, L. J. Roberts and H. Ischiropoulos, *Free Radic. Biol. Med.*, 2012, **52**, 1–6.
47 A. Kellett, Z. Molphy, C. Slator, V. McKee and N. P. Farrell, *Chem. Soc. Rev.*, 2019, **48**, 971–988.
48 J. Madureira, C. I. V. Ramos, M. Marques, C. Maia, B. De Sousa, L. Campino, M. G. Santana-Marques and N. Farrell, *Inorg. Chem.*, 2013, **52**, 8881–8894.
49 Y. Guan, W. Zhou, X. Yao, M. Zhao and Y. Li, *Anal. Chim. Acta*, 2006, **570**, 21–28.
50 J. C. Peberdy, J. Malina, S. Khalid, M. J. Hannon and A. Rodger, *J. Inorg. Biochem.*, 2007, **101**, 1937–1945.
51 M. Zaki, F. Arjmand and S. Tabassum, *Inorganica Chim. Acta*, 2016, **444**, 1–22.
52 D. Branzei and M. Foiani, *Nat. Rev. Mol. Cell Biol.*, 2010, **11**, 208–219.
53 J. C. Wang, *Nat. Rev. Mol. Cell Biol.*, 2002, **3**, 430–440.
54 G. Pistritto, D. Trisciuoglio, C. Ceci, Alessia Garufi and G. D'Orazi, *Aging (Albany. NY).*, 2016, **8**, 603–619.
55 A. Erxleben, *Curr. Med. Chem.*, 2019, **26**, 694–728.
56 P. J. Barnard and S. J. Berners-Price, *Coord. Chem. Rev.*, 2007, **251**, 1889–1902.
57 J. L. Hickey, R. A. Ruhayel, P. J. Barnard, M. V. Baker, S. J. Berners-Price and A. Filipovska, *J. Am. Chem. Soc.*, 2008, **130**, 12570–12571.
58 F. A. Serrano, A. L. Matsuo, P. T. Monteforte, A. Bechara, S. S. Smaili, D. P. Santana, T. Rodrigues, F. V. Pereira, L. S. Silva, J. Machado, E. L. Santos, J. B. Pesquero, R. M. Martins, L. R. Travassos, A. C. F. Caires and E. G. Rodrigues, *BMC Cancer*, 2011, **11**, 296–312.
59 S. J. Berners-Price and A. Filipovska, *Aust. J. Chem.*, 2008, **61**, 661–668.
60 V. Gandin, A. P. Fernandes, M. P. Rigobello, B. Dani, F. Sorrentino, F. Tisato, M. Björnstedt, A. Bindoli, A. Sturaro, R. Rella and C. Marzano, *Biochem. Pharmacol.*, 2010, **79**, 90–101.
61 B. Bertrand and A. Casini, *Dalt. Trans.*, 2014, **43**, 4209–4219.
62 A. Bindoli, M. P. Rigobello, G. Scutari, C. Gabbiani, A. Casini and L. Messori, *Coord. Chem. Rev.*, 2009, **253**, 1692–1707.
63 V. Gandin and A. P. Fernandes, *Molecules*, 2015, **20**, 12732–12756.
64 R. Rubbiani, E. Schuh, A. Meyer, J. Lemke, J. Wimberg, N. Metzler-Nolte, F. Meyer, F. Mohr and I. Ott, *Medchemcomm*, 2013, **4**, 942–948.
65 V. Scalcon, A. Bindoli and M. P. Rigobello, *Free Radic. Biol. Med.*, 2018, **127**, 62–79.
66 C. H. Wang, W. C. Shih, H. C. Chang, Y. Y. Kuo, W. C. Hung, T. G. Ong and W. S. Li, *J. Med. Chem.*, 2011, **54**, 5245–5249.
67 S. J. Allison, M. Sadiq, E. Baronou, P. A. Cooper, C. Dunnill, N. T. Georgopoulos, A. Latif, S. Shepherd, S. D. Shnyder, I. J. Stratford, R. T. Wheelhouse, C. E. Willans and R. M. Phillips, *Cancer Lett.*, 2017, **403**, 98–107.
68 M. Han, M. R. Vakili, H. Soleymani Abyaneh, O. Molavi, R. Lai and A. Lavasanifar, *Mol. Pharm.*, 2014, **11**, 2640–2649.
69 C. Santini, M. Pellei, G. Papini, B. Morresi, R. Galassi, S. Ricci, F. Tisato, M. Porchia, M. P. Rigobello, V. Gandin and C. Marzano, *J. Inorg. Biochem.*, 2011, **105**, 232–240.
70 I. Landini, L. Massai, D. Cirri, T. Gamberi, P. Paoli, L. Messori, E. Mini and S. Nobili, *J. Inorg. Biochem.*, 2020, **208**, 111079.
71 A. B. De Oliveira, B. R. S. Feitosa, C. Näther and I. Jess, *Acta Crystallogr. Sect. E Struct. Reports Online*, 2013, **69**, o1861.
72 Agilent, *CrysAlisPro*, Agilent Technologies Ltd: Yarnton, Oxfordshire, England, 2014.
73 G. M. Sheldrick, *Acta Crystallogr. Sect. A Found. Crystallogr.*, 2008, **64**, 112–122.
74 G. M. Sheldrick, *Acta Crystallogr. Sect. C Struct. Chem.*, 2015, **71**, 3–8.
75 O. V. Dolomanov, L. J. Bourhis, R. J. Gildea, J. A. K. Howard and H. Puschmann, *J. Appl. Crystallogr.*, 2009, **42**, 339–341.
76 C. F. MacRae, I. Sovago, S. J. Cottrell, P. T. A. Galek, P. McCabe, E. Pidcock, M. Platings, G. P. Shields, J. S. Stevens, M. Towler and P. A. Wood, *J. Appl. Crystallogr.*, 2020, **53**, 226–235.